

# X-ray Diffraction Analysis and Conformational Energy Computations of $\beta$ -Turn and $3_{10}$ -Helical Peptides Based on $\alpha$ -Amino Acids with an Olefinic Side Chain. Implications for Ring-Closing Metathesis

Michele Saviano and Ettore Benedetti

Biocrystallography Research Center, C.N.R., Department of Chemistry, University of Naples "Federico II", 80134 Naples, Italy

Rosa Maria Vitale

Department of Environmental Sciences, 2<sup>nd</sup> University of Naples, 81100 Caserta, Italy

Bernard Kaptein and Quirinus B. Broxterman

DSM Fine Chemicals, Advanced Synthesis and Catalysis, P.O. Box 18, 6160 MD Geleen, The Netherlands

Marco Crisma, Fernando Formaggio, and Claudio Toniolo\*

Biopolymer Research Center, C.N.R., Department of Organic Chemistry, University of Padova, 35131 Padova, Italy

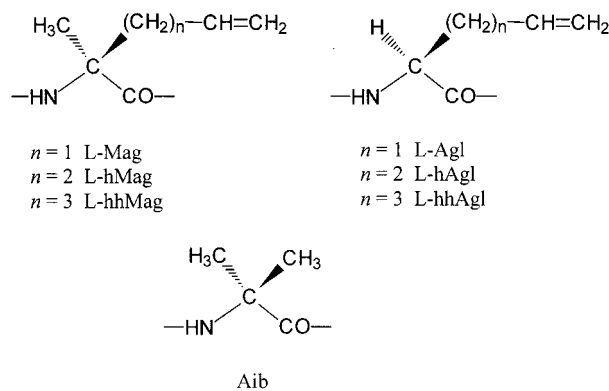
Received November 26, 2001; Revised Manuscript Received February 27, 2002

**ABSTRACT:** We describe the X-ray diffraction structure of the terminally protected dipeptide amide Boc-Aib-L-Mag-NHBzl (Aib is  $\alpha$ -aminoisobutyric acid and Mag is C $^{\alpha}$ -methyl, C $^{\alpha}$ -allyl-glycine) and the results of conformational energy computations on Ac-L-Mag-NHMe, Ac-Aib-L-Mag-NHMe, and Ac-L-Mag-Aib-NHMe. On the basis of these data, we performed conformational energy computations on the sequence -Aib-Xxx-(Aib)<sub>2</sub>-Xxx-Aib- (Xxx = L-Mag) to check the feasibility of ring-closing metathesis, a currently extensively investigated reaction useful to enhance peptide helicity and metabolic stability, on this  $3_{10}$ -helix forming model hexamer with the two olefinic amino acids at the  $i, i+3$  relative positions. Computations were extended to peptides based on olefinic residues with the side chains elongated by one (L-hMag) or two (L-hhMag) carbon atoms. A comparison was also made with peptides characterized by the related, non-C $^{\alpha}$ -methylated (C $^{\alpha}$ -trisubstituted) L-Agl (C $^{\alpha}$ -allyl-L-glycine), L-hAgl, and L-hhAgl residues. We conclude that, to achieve ring-closing metathesis with an unperturbed  $3_{10}$ -helical conformation and a symmetrical all-hydrocarbon tether, the side-chain length for each of the two  $i, i+3$  olefinic amino acids requires at least five carbon atoms (hhMag or hhAgl), thereby producing an 18-atom macrocycle.

## Introduction

An intramolecular side-chain to side-chain covalent bond between two amino acids in a peptide chain results in the formation of a well-defined loop. In particular, if the number of intervening residues is small (<4), the cyclic structure formed will enjoy a limited conformational flexibility. This property, in turn, may increase receptor binding affinity and selectivity, reduce enzymatic degradation rate and immunogenicity, and make peptidomimetic drug design easier. Among the biologically stable covalent bonds the appealing all-hydrocarbon aliphatic tether can be formed by the powerful ring-closing metathesis (RCM) methodology developed by Grubbs (for recent review articles see refs 1–5). In this connection, (i) Verdine and co-workers<sup>6</sup> experimentally screened L- and D-amino acid configurations and side-chain lengths (from 3 to 8 carbon atoms) of olefinic residues in the RCM reaction of terminally blocked, 15-mer  $\alpha$ -helical peptides. The two olefinic amino acids were set at  $i, i+4$  or  $i, i+7$  relative positions, i.e., after one or two complete turns, respectively, of the  $\alpha$ -helical structure (characterized by 3.6 residues per turn).<sup>7</sup> In particular, in the case of two L-residues at the  $i, i+4$

positions, the smallest macrocycle formed has 20 atoms. (ii) Grubbs and co-workers<sup>8,9</sup> have efficiently metathesized two terminally protected, 7-mer,  $3_{10}$ -helical<sup>7</sup> peptides with two olefinic L-residues of 5 or 6 side-chain atoms each, located at the  $i, i+4$  positions. Macrocyclizations produced ring systems of 21 and 23 atoms, respectively. In these studies the short helical structures were induced by C $^{\alpha}$ -methylated  $\alpha$ -amino acids, either Mag (C $^{\alpha}$ -methyl, C $^{\alpha}$ -allylglycine)<sup>10–13</sup> and its higher homologues or Aib ( $\alpha$ -aminoisobutyric acid or C $^{\alpha,\alpha}$ -dimethylglycine).<sup>14,15</sup>



\* To whom correspondence should be addressed. Tel (+39) 049-827-5247; Fax (+39) 049-827-5239; e-mail claudio.toniolo@unipd.it.

Recently, by a chemo-enzymatic approach, we performed a large-scale synthesis of Mag and experimentally investigated the preferred conformations of a variety of Mag-rich model peptides.<sup>10–13</sup> We found that this C $^{\alpha}$ -tetrasubstituted  $\alpha$ -amino acid, as its prototype Aib,<sup>14,15</sup> is an excellent  $\beta$ -turn<sup>16–18</sup> and  $3_{10}$ -helix former (the  $3_{10}$ -helix is generated by a series of consecutive type III or type III'  $\beta$ -turns).<sup>7</sup> In particular, a peptide with two Mag residues, one on top of the other after a complete turn of the  $3_{10}$ -helix, was crystallographically characterized.

In this work we first deepened our knowledge of the turn conformational preferences of the -Mag-Aib- and -Aib-Mag- dipeptide sequences by carrying out an X-ray diffraction analysis of Boc-Aib-L-Mag-NHBzl (Boc, *tert*-butyloxycarbonyl; NHBzl, benzylamino) and conformational energy calculations on Ac-L-Mag-NHMe (Ac, acetyl; NHMe, methylamino), Ac-L-Mag-Aib-NHMe, and Ac-Aib-L-Mag-NHMe. Second, on the basis of the conclusions from our experimental approach, we theoretically investigated the feasibility to produce macrocycles via olefin RCM on terminally blocked, unperturbed  $3_{10}$ -helical hexapeptides with the common sequence Ac-Aib-Xxx-(Aib)<sub>2</sub>-Xxx-Aib-NHMe, where the Xxx residues incorporated at the *i*, *i*+3 positions, i.e., after one complete turn of the ternary helix, are either two C $^{\alpha}$ -methylated, olefinic L-residues (Mag, hMag, hhMag) or two of their non-C $^{\alpha}$ -methylated L-counterparts (Agl, hAgl, hhAgl).

## Experimental Section

**Synthesis of Peptides.** The synthesis and characterization of the dipeptide Boc-Aib-L-Mag-NHBzl have already been reported.<sup>12</sup>

**X-ray Diffraction.** Colorless crystals of Boc-Aib-L-Mag-NHBzl were grown from methanol by slow evaporation. Data collection was performed on a Philips PW1100 four-circle diffractometer. Intensities were corrected for Lorentz and polarization effects. No absorption correction was made. The structure was solved by direct methods of the SHELXS 97 program.<sup>19</sup> Refinement was carried out by full-matrix-block least-squares on  $F^2$ , using all data, with all non-H atoms anisotropic, by application of the SHELXL 97 program,<sup>20</sup> allowing the positional parameters and the anisotropic displacement parameters of the non-H atoms to refine at alternate cycles. H atoms of the dipeptide molecule were calculated at idealized positions and refined as riding with  $U_{iso}$  set equal to 1.2 (or 1.5 for the methyl group) times the  $U_{eq}$  of the parent atom. Crystallographic data and structure refinement parameters are listed in Table 1.

Crystallographic data (excluding structure factors) for the structure reported in this paper have been deposited as Supporting Information.

**Conformational Energy Computations.** Energy calculations were initially carried out on Ac-L-Mag-NHMe. The geometries of the acetamido and methylamido N- and C-blocking groups were those proposed by Scheraga, Némethy, and co-workers.<sup>21,22</sup> Conformational energy calculations were performed using the INSIGHT/DISCOVER package<sup>23</sup> with the Consistent Valence Force Field (CVFF).<sup>24–26</sup> A dielectric constant of 1 was assumed in all calculations. The conformational space was mapped by calculating the conformational energy at 18° intervals for the  $\phi, \psi$  backbone torsion angles and by computing energy maps at six pairs of side-chain  $\chi^1$  and  $\chi^2$  torsion angles (60°, 120°; 60°, -120°; -60°, -120°; -60°, 120°; 180°, 120°; 180°, -120°). These angles were selected from an analysis of the X-ray structures of Mag-containing peptides reported in the literature<sup>10,11</sup> and in the present work. More specifically, out of the 16 Mag side-chain conformations found in the crystal state, two have the 60°, 120° pair; three have the 60°, -120° pair; five have the -60°, -120° pair; two have

**Table 1. Crystal Data and Structure Refinement Parameters for Boc-Aib-L-Mag-NHBzl**

empirical formula	C <sub>22</sub> H <sub>33</sub> N <sub>3</sub> O <sub>4</sub>
formula weight	403.51
temp, K	293(2)
wavelength, Å	1.54178 (Cu K $\alpha$ )
crystal system, space group	orthorhombic, $P2_12_12_1$
unit cell dimensions	$a = 5.897(2)$ Å $b = 17.248(3)$ Å $c = 23.016(4)$ Å
vol, Å <sup>3</sup>	2341(1)
Z; calculated density, Mg/m <sup>3</sup>	4; 1.145
absorption coeff, mm <sup>-1</sup>	0.638
$F(000)$	872
crystal size, mm <sup>3</sup>	0.50 $\times$ 0.50 $\times$ 0.30
scan mode	$\theta$ - $2\theta$
$\theta$ range for data collection, deg	5.48–59.89
limiting indices	$-1 \leq h \leq 6, 0 \leq k \leq 19, 0 \leq l \leq 25$
reflections collected/unique	2435/2392 [ $R(\text{int}) = 0.0167$ ]
refinement method	full-matrix-block least-squares on $F^2$
data/restraints/parameters	2392/13/251
goodness-of-fit on $F^2$	1.033
final $R$ indices [ $I \geq 2\sigma(I)$ ]	$R_1 = 0.0369, wR_2 = 0.1043$
$R$ indices (all data)	$R_1 = 0.0385, wR_2 = 0.1064$
largest diff peak and hole, e Å <sup>-3</sup>	0.162 and -0.186

the -60°, 120° pair; four have the 180°, 120° pair; and none has the 180°, -120° pair (despite the fact that this theoretically accessible, last pair of torsion angles has not been experimentally found, at least to date, we did compute the related energy map for torsion angle symmetry completeness). In all search the  $\omega$  torsion angles were fixed at 180°. The terminal methyl groups were frozen into staggered conformations.<sup>27</sup> Minimum-energy conformations were obtained in the low-energy regions located in the above searches by minimizing the energy with respect to all geometrical parameters using the conjugate gradient algorithm.<sup>28</sup> All conformational energies are expressed as  $\Delta E = E - E_0$  where  $E_0$  is the energy of the most stable conformation.

Rigid-rotor maps were subsequently obtained for the Ac-Aib-L-Mag-NHMe and Ac-L-Mag-Aib-NHMe terminally blocked peptides, setting Aib at  $\phi = -60^\circ, \psi = -30^\circ$  or at  $\phi = 60^\circ, \psi = 30^\circ$  (the  $3_{10}$ -helical, largely preferred conformations for this residue<sup>14,15</sup>) and the Mag side-chain conformations as described above. After this first step, minimum-energy conformations were obtained in the low-energy regions located in the above searches by minimizing the energy with respect to all Mag geometrical parameters using the conjugate gradient algorithm.

Conformational energy computations were finally carried out on the Ac-Aib-Xxx-(Aib)<sub>2</sub>-Xxx-Aib-NHMe terminally blocked hexapeptide amides with Xxx = L-Mag, L-hMag, L-hhMag or L-Agl, L-hAgl, and L-hhAgl. All peptides were generated with the module BIOPOLYMER available in the INSIGHT II/DISCOVER package. The starting geometry was fixed to a canonical  $3_{10}$ -helix ( $\phi = -60^\circ, \psi = -30^\circ$ ). The side chains of the olefinic residues in each peptide were cyclized by RCM, and the energy was subsequently minimized in two steps: in the first cycle constraints were applied on the backbone H-bonding to adjust the macrocyclic ring without distortion of the helical conformation, and in the second step the constraints were removed to allow a full minimization. All the minimizations were performed in vacuo with the AMBER force field,<sup>29</sup> using the conjugate gradient algorithm and a dielectric constant of 1. All computations were performed on a Silicon Graphics Octane workstation of the Biocrystallography Research Centre (CNR) at Naples.

## Results and Discussion

**Crystal-State Conformation.** We determined by X-ray diffraction the crystal structure of the terminally protected dipeptide amide Boc-Aib-L-Mag-NHBzl. The molecular structure with the atomic numbering scheme

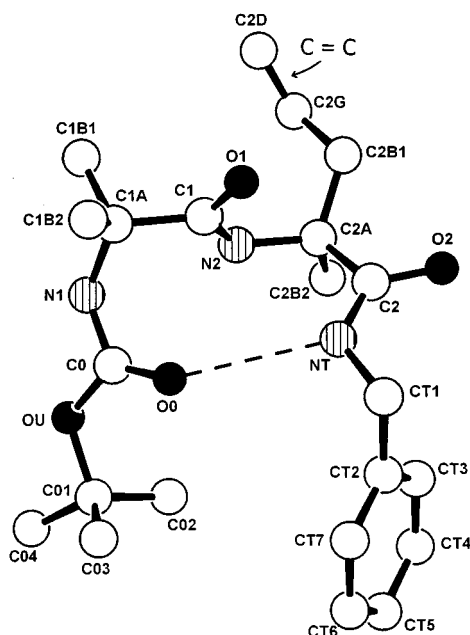


**Figure 1.** X-ray diffraction structure of Boc-Aib-L-Mag-NHBzl with numbering of the atoms. The intramolecular H-bond is represented by a dashed line.

is shown in Figure 1. This is the second crystal-state structure solved for an Aib/Mag peptide after the tripeptide Boc-Aib-L-Mag-Aib-OMe.

Bond lengths and bond angles (deposited) are in general agreement with previously reported values for the geometry of the *tert*-butyloxycarbonyl-amino urethane<sup>30</sup> and amide<sup>31</sup> moieties, the Aib<sup>32,33</sup> and Mag<sup>10,11</sup> residues, and the peptide unit.<sup>34,35</sup> In particular, the bond distances and bond angle for the Mag side-chain allyl moiety are as follows: C2D=C2G, 1.288(4) Å; C2G–C2B1, 1.490(4) Å; and C2D=C2G–C2B1, 123.8(5)°. The corresponding literature mean values for the H<sub>2</sub>C=CH– and =CH–CH<sub>2</sub>– distances are 1.30 and 1.50 Å, respectively.<sup>36</sup> Also, the Mag bond angles indicate an asymmetric geometry for the C<sup>α</sup> atom. More specifically, the bond angles involving the C2B1 atom are wider (by 4–5°) than those involving the C2B2 atom. This observation is common to other C<sup>α</sup>-tetrasubstituted α-amino acids.<sup>15,37</sup> The value for the conformationally sensitive N2–C2A–C2 (τ) bond angle is 111.9(2)°, comparable to that exhibited by the other C<sup>α</sup>-tetrasubstituted α-amino acids forming bends and helices.<sup>15,32</sup>

Both the achiral Aib and the L-Mag residues are found in the helical region (A\*) of the conformational map.<sup>27</sup> The backbone  $\phi, \psi$  torsion angles are  $\phi_1 = 55.7(3)^\circ$ ,  $\psi_1 = 33.1(3)^\circ$ ,  $\phi_2 = 64.7(3)^\circ$ , and  $\psi_2 = 22.5(3)^\circ$ .<sup>38</sup> As a result, the -Aib-L-Mag- sequence is folded in a 1 ← 4 C'=O ... H–N intramolecularly H-bonded β-turn conformation of the left-handed helical (III') type. The C0=O0...NT intramolecular separation, 2.932(2) Å, is within the limits expected for such H-bonds.<sup>39–41</sup> It is worth recalling that both crystallographically independent molecules in the asymmetric unit of Boc-Aib-L-Mag-Aib-OMe were found to be folded in a β-turn conformation, but they have opposite handedness.<sup>10</sup> In summary, a single L-Mag residue tends to be helical, but it is not able to induce a clear-cut bias for any of the two screw senses.

Two out of the three  $\omega$  torsion angles ( $\omega_0$  and  $\omega_2$ ) significantly deviate ( $|\Delta\omega| > 10^\circ$ ) from the ideal value of the trans-planar urethane, peptide, and amide units

(180°). The trans arrangement of the  $\theta^1$  torsion angle of the Boc-NH– moiety, 164.6(2)°, is that commonly reported for N-terminal Boc-protected peptides (type *b* conformation).<sup>30</sup> In the L-Mag residue the side-chain N2–C2A–C2B1–C2G ( $\chi^1$ ) torsion angle is in the *g* conformation, –53.4(4)°, while the C2A–C2B1–C2G–C2D ( $\chi^2$ ) torsion angle is 123.4(4)°. In our previous X-ray diffraction analysis of Mag peptides we reported no evident side-chain conformation bias for the  $\chi^1$  angle, whereas the  $\chi^2$  angle was consistently found in the rather restricted range  $\pm 110$ –130° (*skew* conformation).<sup>10,11</sup>

The packing mode of the Boc-Aib-L-Mag-NHBzl molecules is characterized by one intermolecular H-bond between the urethane N–H group of the Aib residue and the amide C'=O group of the Mag residue. The N1...O2=C2 ( $1 - x, \frac{1}{2} + y, \frac{1}{2} - z$ ) intermolecular distance is 3.023(2) Å (Figure 2). This H-bond gives rise to rows of molecules along the *b*-direction. The crystal structure is further stabilized by van der Waals interactions among the benzyl aromatic and the *tert*-butyl and allyl aliphatic groups along the other crystallographic directions.

**Conformational Energy Computations.** To examine the conformational preferences of the Mag residue, theoretical calculations on Ac-L-Mag-NHMe were carried out at the six pairs of values for the side-chain  $\chi^1$  and  $\chi^2$  torsion angles 60°, 120°; 60°, –120°; –60°, –120°; –60°, 120°; 180°, 120°; 180°, –120° (see Experimental Section). A typical rigid rotor ( $\phi, \psi$ ) map for a pair of  $\chi^1$  and  $\chi^2$  angles (60°, 120°) is illustrated in Figure 3.

An inspection of the maps shows a dependence of the backbone geometry on the side-chain torsion angles. In particular, a comparative analysis of the maps (Tables 2–7) reveals that the lowest energy backbone conformation having  $\chi^1 = 60^\circ$ ,  $\chi^2 = 120^\circ$  (Table 2) and  $\chi^1 = 60^\circ$ ,  $\chi^2 = -120^\circ$  (Table 3) is the fully extended (180°, 180°) conformation,<sup>17</sup> followed by the quasi-extended (180°, 54°; –72°, 180°; and 180°, –36°), inverse  $\gamma$ -turn<sup>17,42</sup> (–72°, 54°), and right-handed helical<sup>7</sup> (–72°, –36°) domains. Interestingly, when  $\chi^1 = -60^\circ$ ,  $\chi^2 = -120^\circ$  or  $\chi^1 = -60^\circ$ ,  $\chi^2 = 120^\circ$  (Tables 4 and 5), the propensity is opposite: the right- and left-handed helical and inverse  $\gamma$ -turn conformations are preferred compared with the quasi-extended conformations (the extended conformation is not a minimum). The low-energy state having  $\chi^1 = 180^\circ$ ,  $\chi^2 = 120^\circ$  (Table 6) is quasi-extended, followed by the  $\gamma$ -turn, extended and left-handed helical conformations. The low-energy domains having  $\chi^1 = 180^\circ$ ,  $\chi^2 = -120^\circ$  (Table 7) are the quasi-extended and extended conformations, followed by the helical and  $\gamma$ -turn conformations. It is noteworthy that  $\chi^1$  is more influential on the backbone geometry than  $\chi^2$ , as shown by the maps that are quite similar when  $\chi^1$  has the same value.

The application of the full minimization procedures to these low-energy conformations confirms the dependence of  $\phi, \psi$  on  $\chi^1$  and the remarkably more limited influence of  $\chi^2$ . In particular, the minimum-energy conformations in the maps represent the  $\gamma$ -turn (lowest energy) and helical conformations for  $\chi^1$  equal to  $\pm 60^\circ$  and 180°, respectively. However, in all cases the energy of the helical conformations is close to the minimum, thus indicating that they are easily accessible and that the  $\phi, \psi$  bias induced by  $\chi^1$  is not strong. These theoretical findings agree well with the results of the X-ray analysis (see Experimental Section).



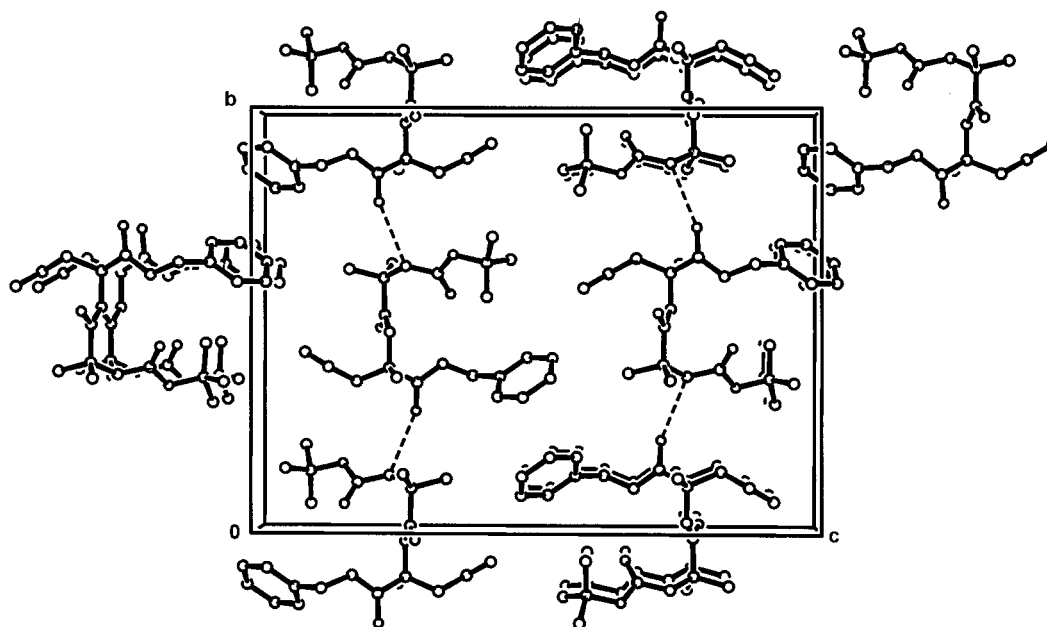


**Figure 2.** Mode of crystal packing of the Boc-Aib-L-Mag-NHBzl molecules along the *a*-direction. Intermolecular H-bonds are represented by dashed lines.

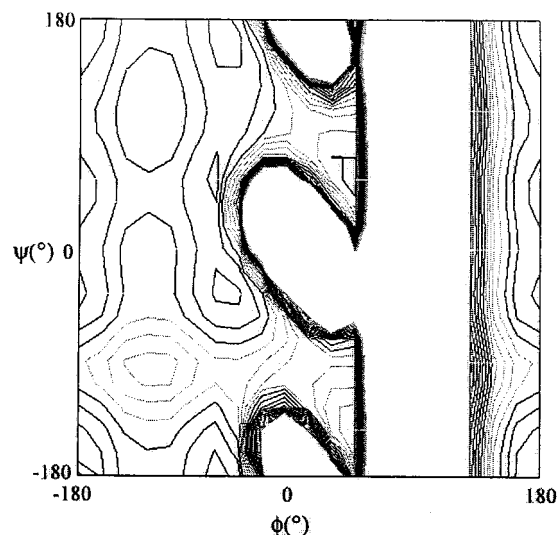


**Figure 3.** Rigid-rotor ( $\phi$ ,  $\psi$ ) map of Ac-L-Mag-NHMe with the side-chain  $\chi^1$  and  $\chi^2$  torsion angles set to  $60^\circ$ ,  $120^\circ$ .

**Table 2. Minimum-Energy Conformations from the Rigid-Rotor Map of Ac-L-Mag-NHMe ( $\chi^1 = 60^\circ$ ,  $\chi^2 = 120^\circ$ )**

$\phi$ (deg)	$\psi$ (deg)	$\Delta E$ (kcal/mol)
180	180	0.0
180	-162	1.0
180	162	1.8
180	54	3.9
-72	180	4.6
180	-36	5.4
-72	54	5.4
-72	-36	6.1

With the aim at investigating the conformational preference of the Mag residue when it is preceded or followed by a helicogenic residue (Aib), we calculated rigid rotor maps for Ac-Aib-L-Mag-NHMe (this sequence corresponds to the dipeptide X-ray structure described above) and Ac-L-Mag-Aib-NHMe (see Experimental Section). When the Aib residue is fixed in the right-handed helical conformation, the lowest energy conformation for the Mag residue in these maps is the  $\gamma$ -turn

**Table 3. Minimum-Energy Conformations from the Rigid-Rotor Map of Ac-L-Mag-NHMe ( $\chi^1 = 60^\circ$ ,  $\chi^2 = -120^\circ$ )**

$\phi$ (deg)	$\psi$ (deg)	$\Delta E$ (kcal/mol)
180	180	0.0
180	54	3.2
-72	180	4.0
-72	54	4.1
-54	162	5.6
180	-36	6.1
-72	-36	6.2

**Table 4. Minimum-Energy Conformations from the Rigid-Rotor Map of Ac-L-Mag-NHMe ( $\chi^1 = -60^\circ$ ,  $\chi^2 = -120^\circ$ )**

$\phi$ (deg)	$\psi$ (deg)	$\Delta E$ (kcal/mol)
-72	-72	0.0
54	54	0.6
-72	54	1.6
-54	-54	1.9
54	-162	3.5
-72	180	4.2

**Table 5. Minimum-Energy Conformations from the Rigid-Rotor Map of Ac-L-Mag-NHMe ( $\chi^1 = -60^\circ$ ,  $\chi^2 = 120^\circ$ )**

$\phi$ (deg)	$\psi$ (deg)	$\Delta E$ (kcal/mol)
-72	72	0.0
54	54	0.9
-54	-54	1.5
-54	-162	1.9
54	-162	4.1
-72	180	4.4

(Table 8). However, the energy of the right-handed helical conformation is close to the minimum. When Aib is switched to the left-handed helical domain, it is the most stable also for the Mag residue.

Finally, to determine the minimal side-chain length required by two olefinic residues at the *i*, *i*+3 relative positions to produce stable macrocycles on an unperturbed  $3_{10}$ -helix via RCM, peptides of the type Ac-Aib-Xxx-(Aib)<sub>2</sub>-Xxx-Aib-NHMe (Xxx = L-Mag, L-hMag and L-hhMag or L-Agl, L-hAgl and L-hhAgl) were theoretically analyzed. The results of the energy minimization study for the C $^\alpha$ -methylated series indicate that two

**Table 6. Minimum-Energy Conformations from the Rigid-Rotor Map of Ac-L-Mag-NHMe ( $\chi^1 = 180^\circ$ ,  $\chi^2 = 120^\circ$ )**

$\phi$ (deg)	$\psi$ (deg)	$\Delta E$ (kcal/mol)
180	-54	0.0
54	-54	1.0
180	72	1.1
-72	72	1.2
180	162	1.7
54	72	2.7
54	-90	4.1

**Table 7. Minimum-Energy Conformations from the Rigid-Rotor Map of Ac-L-Mag-NHMe ( $\chi^1 = 180^\circ$ ,  $\chi^2 = -120^\circ$ )**

$\phi$ (deg)	$\psi$ (deg)	$\Delta E$ (kcal/mol)
180	-54	0.0
180	162	0.9
-54	-54	1.0
180	72	1.8
-72	-90	2.0
54	72	3.5
54	-90	4.6

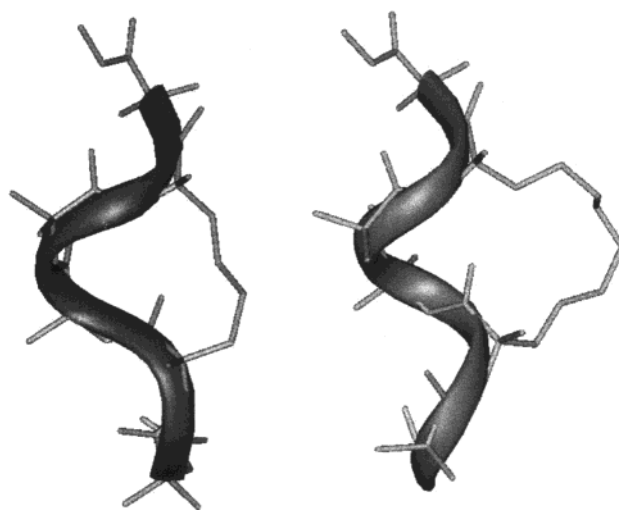
**Table 8. Minimum-Energy Conformations for Ac-Aib-L-Mag-NHMe and Ac-L-Mag-Aib-NHMe**

compound	Aib		L-Mag		$\Delta E$ (kcal/mol)
	$\phi$ (deg)	$\psi$ (deg)	$\phi$ (deg)	$\psi$ (deg)	
Ac-Aib-L-Mag-NHMe	-60	-30	73	-58	0.0
			-52	-27	1.0
			-68	57	2.3
	60	30	60	20	0.0
			72	-50	1.0
Ac-L-Mag-Aib-NHMe	-60	-30	-74	61	1.3
			71	-67	0.0
			-56	-11	1.1
	60	30	-69	63	2.0
			65	-67	3.7
			62	22	0.0
			-63	81	1.1
			-174	-61	5.1

five-carbon side chains, such as those present in L-hhMag, are the shortest to give macrocyclization without perturbation of the  $3_{10}$ -helix (Table 9 and Figure 4). Strictly comparable data were obtained for the related non-C $^\alpha$ -methylated series, where only the bis L-hhAgl containing, N $^\alpha$ -acetylated hexapeptide methylamide macrocyclized without helical distortion.

## Conclusions

Verdine and co-workers<sup>6</sup> clearly demonstrated that it is possible to cyclize via RCM a unperturbed  $\alpha$ -helical peptide at both  $i$ ,  $i+4$  and  $i$ ,  $i+7$  relative positions provided that the olefinic side chains have an appropriate length. In an all-L peptide, if both olefinic residues at the  $i$ ,  $i+4$  positions are of either the L- or the D-configuration, the smallest ring system formed has 20 atoms. Moreover, in an all-L peptide, if the olefinic residues at the  $i$ ,  $i+7$  positions are one of the L- and

**Figure 4.** Minimum-energy models for the two hexapeptides Ac-Aib-Xxx-(Aib)<sub>2</sub>-Xxx-Aib-NHMe with the ( $i$ ,  $i+3$ ) Xxx residues L-Mag (HP1), left part, or L-hhMag (HP3), right part.

the other of the D-configuration, the smallest ring system formed has 31 atoms.

Grubbs and co-workers<sup>8,9</sup> synthesized cyclic peptides of 21 and 23 atoms in high yields via RCM of two olefinic L-residues located at the  $i$ ,  $i+4$  positions. The  $3_{10}$ -helical structure of the peptide reagent seems to be preserved in the cyclic product. However, it is worth pointing out that in a  $3_{10}$ -helix the intramolecular distance between residues  $i$  and  $i+4$  is significantly higher than the  $i$ ,  $i+3$  distance.

Interestingly, a 19-atom ring system with an all -CH<sub>2</sub>- tether was recently prepared joining the side chains of two L-residues at the  $i$ ,  $i+4$  positions by a novel route *not* involving RCM.<sup>43</sup> However, the resulting cyclic peptide does not adopt a helical conformation.

In the aforementioned Verdine<sup>6</sup> and Grubbs<sup>8,9</sup> peptides, both olefinic residues are *internal* to the helical systems. Grubbs and co-workers<sup>44</sup> were also able to cyclize via RCM three peptides forming one or two consecutive  $\beta$ -turns, each with two Agl ( $i$ ,  $i+3$ ) residues. The resulting cyclic system is small (14 atoms). Analogous results were reported by our group<sup>12</sup> with a turn-forming, Agl/Mag  $i$ ,  $i+3$  peptide and by Blachert and co-workers.<sup>45</sup> It is very important to note that in all these cases the N-terminal C $^\alpha$ -trisubstituted Agl (or related) residue is *outside* the rigid, central  $\beta$ -turn structure. We also reported the failure to achieve RCM in several  $\beta$ -turn/ $3_{10}$ -helical, Mag/Mag  $i$ ,  $i+3$  peptides (in these compounds both Mag residues are internal to the turns/helices), i.e., the 14-atom ring system is not formed. At this point, it is relevant to mention that in the crystal state the Cys1 residue of the related, disulfide tethered Boc-Cys-Pro-Aib-Cys-NHMe peptide, that also forms a 14-atom ring system, is *outside* the two consecutive  $\beta$ -turn structure.<sup>46</sup>

**Table 9. Minimum-Energy Conformations for the Three RCM Macrocyclized Peptides from Ac-Aib-Xxx-(Aib)<sub>2</sub>-Xxx-Aib-NHMe with Xxx = L-Mag, L-hMag, and L-hhMag**

HP1	$\phi$ (deg)	$\psi$ (deg)	HP2	$\phi$ (deg)	$\psi$ (deg)	HP3	$\phi$ (deg)	$\psi$ (deg)
Aib	-46.5	-47.1	Aib	-41.1	-31.7	Aib	-38.3	-41.4
Mag	-65.4	48.6 <sup>a</sup>	hMag	-43.8	-42.0	hhMag	-41.7	-34.5
Aib	-49.4	-52.1	Aib	57.2 <sup>a</sup>	-74.9	Aib	-38.8	-30.0
Aib	-57.4	-27.3	Aib	-45.1	-37.5	Aib	-36.5	-34.3
Mag	-51.8	-33.5	hMag	-40.7	-35.5	hhMag	-38.4	-38.2
Aib	-51.0	-30.4	Aib	-62.0	-30.9	Aib	-51.7	-29.2

<sup>a</sup> Severe helix distortion.

In the present paper, in addition to experimentally and theoretically confirming the  $\beta$ -turn propensity for the allyl-based C $^{\alpha}$ -tetrasubstituted  $\alpha$ -amino acid Mag, our conformational energy computations significantly expanded the picture of RCM in turn/helical peptides by indicating that two  $i, i+3$  side chains of the type  $-(CH_2)_3-CH=CH_2$  (hhMag or hhAgl) represent the minimal length requirement to achieve RCM on an unperturbed  $3_{10}$ -helix. In these compounds 18-atom ring systems are formed. It is gratifying that these findings indirectly support Grubbs,<sup>44</sup> Blechert,<sup>45</sup> and our<sup>12</sup> experimental results discussed above.

**Supporting Information Available:** Tables giving crystal data and structure refinement information, atomic coordinates and equivalent isotropic displacement parameters, anisotropic displacement parameters, hydrogen atom coordinates, bond distances, bond angles, torsion angles, and hydrogen bond data for the X-ray diffraction structure of Boc-Aib-L-Mag-NHBzl. This material is available free of charge via the Internet at <http://pubs.acs.org>.

## References and Notes

- Grubbs, R. H.; Chang, S. *Tetrahedron* **1998**, *54*, 4413.
- Armstrong, S. K. *J. Chem. Soc., Perkin Trans. 1* **1998**, 371.
- Phillips, A. J.; Abell, A. D. *Aldrichim. Acta* **1999**, *32*, 75.
- Rutjes, F. P. J. T.; Wolf, L. B.; Schoemaker, H. E. *J. Chem. Soc., Perkin Trans. 1* **2000**, 4197.
- Lambert, J. N.; Mitchell, J. P.; Robert, K. D. *J. Chem. Soc., Perkin Trans. 1* **2001**, 471.
- Schafmeister, C. E.; Verdine, G. L. *J. Am. Chem. Soc.* **2000**, *122*, 5891.
- Toniolo, C.; Benedetti, E. *Trends Biochem. Sci.* **1991**, *16*, 350.
- Blackwell, H. E.; Grubbs, R. H. *Angew. Chem., Int. Ed. Engl.* **1998**, *37*, 3281.
- Blackwell, H. E.; Sadowsky, J. D.; Howard, R. J.; Sampson, J. N.; Chao, J. A.; Steinmetz, W. E.; O'Leary, D. J.; Grubbs, R. H. *J. Org. Chem.* **2001**, *66*, 5291.
- Peggion, C.; Flammengo, R.; Mossel, E.; Broxterman, Q. B.; Kaptein, B.; Kamphuis, J.; Formaggio, F.; Crisma, M.; Toniolo, C. *Tetrahedron* **2000**, *56*, 3589.
- Peggion, C.; Formaggio, F.; Crisma, M.; Toniolo, C.; Kamphuis, J.; Kaptein, B.; Broxterman, Q. B.; Vitale, R. M.; Iacovino, R.; Saviano, M.; Benedetti, E. *Macromolecules* **2001**, *34*, 4263.
- Kaptein, B.; Broxterman, Q. B.; Schoemaker, H. E.; Rutjes, F. P. J. T.; Veerman, J. J. N.; Kamphuis, J.; Peggion, C.; Formaggio, F.; Toniolo, C. *Tetrahedron* **2001**, *57*, 6567.
- Toniolo, C.; Crisma, M.; Formaggio, F.; Peggion, C.; Broxterman, Q. B.; Kaptein, B.; Schoemaker, H. E.; Rutjes, F. P. J. T.; Veerman, J. J. N.; Vitale, R. M.; Benedetti, E.; Saviano, M. In *Peptides: The Wave of the Future*; Lebl, M., Houghten, R. A., Eds.; American Peptide Society: San Diego, CA, 2001; pp 371–372.
- Karle, I. L.; Balaram, P. *Biochemistry* **1990**, *29*, 6747.
- Toniolo, C.; Benedetti, E. *Macromolecules* **1991**, *24*, 4004.
- Venkatachalam, C. M. *Biopolymers* **1968**, *6*, 1425.
- Toniolo, C. *C. R. C. Crit. Rev. Biochem.* **1980**, *9*, 1.
- Rose, G. D.; Gierasch, L. M.; Smith, J. P. *Adv. Protein Chem.* **1985**, *37*, 1.
- Sheldrick, G. M. *SHELXS 97. Program for the Solution of Crystal Structures*; University of Göttingen: Göttingen, Germany, 1997.
- Sheldrick, G. M. *SHELXL 97. Program for Crystal Structure Refinement*; University of Göttingen: Göttingen, Germany, 1997.
- Momany, F. A.; McGuire, R. F.; Burgess, A. W.; Scheraga, H. A. *J. Phys. Chem.* **1975**, *79*, 2361.
- Némethy, G.; Pottle, M. S.; Scheraga, H. A. *J. Phys. Chem.* **1983**, *87*, 1883.
- INSIGHT II and DISCOVER User's Guides*; Molecular Simulations Inc.: San Diego, CA, 1999 (release 2000).
- Lifson, S.; Hagler, A. T.; Dauber, P. J. *J. Am. Chem. Soc.* **1979**, *101*, 5111.
- Hagler, A. T.; Lifson, S.; Dauber, P. J. *J. Am. Chem. Soc.* **1979**, *101*, 5122.
- Hagler, A. T.; Dauber, P. J.; Lifson, S. *J. Am. Chem. Soc.* **1979**, *101*, 5131.
- Zimmerman, S. S.; Pottle, M. S.; Némethy, G.; Scheraga, H. A. *Macromolecules* **1977**, *10*, 1.
- Brooks, C. L. III; Pettit, M. B.; Karplus, M. In *Proteins: a Theoretical Perspective of Dynamics, Structure and Thermodynamics*; Wiley: New York, 1988.
- Weiner, S. F.; Kollman, P. A.; Nguyen, D. T.; Case, D. A. *J. Comput. Chem.* **1986**, *7*, 230.
- Benedetti, E.; Pedone, C.; Toniolo, C.; Némethy, G.; Pottle, M. S.; Scheraga, H. A. *Int. J. Pept. Protein Res.* **1980**, *16*, 156.
- Chakrabarti, P.; Dunitz, J. D. *Helv. Chim. Acta* **1982**, *65*, 1555.
- Paterson, Y.; Rumsey, S. M.; Benedetti, E.; Némethy, G.; Scheraga, H. A. *J. Am. Chem. Soc.* **1981**, *103*, 2947.
- Valle, G.; Crisma, M.; Formaggio, F.; Toniolo, C.; Jung, G. *Liebigs Ann. Chem.* **1987**, 1055.
- Benedetti, E. In *Chemistry and Biochemistry of Amino Acids, Peptides and Proteins*; Weinstein, B., Ed.; Dekker: New York, 1982; Vol. 6, pp 105–184.
- Ashida, T.; Tsunogae, Y.; Tanaka, I.; Yamane, T. *Acta Crystallogr.* **1987**, *B43*, 212.
- Allen, F. H.; Kennard, O.; Watson, D. G.; Brammer, L.; Orpen, A. G.; Taylor, R. *J. Chem. Soc., Perkin Trans. 2* **1987**, S1–S19.
- Moretto, V.; Formaggio, F.; Crisma, M.; Bonora, G. M.; Toniolo, C.; Benedetti, E.; Santini, A.; Saviano, M.; Di Blasio, B.; Pedone, C. *J. Pept. Sci.* **1996**, *2*, 14.
- IUPAC-IUB Commission on Biochemical Nomenclature; *J. Mol. Biol.* **1970**, *52*, 1.
- Ramakrishnan, C.; Prasad, N. *Int. J. Protein Res.* **1971**, *3*, 209.
- Taylor, R.; Kennard, O.; Versichel, W. *Acta Crystallogr.* **1984**, *B40*, 280.
- Görbitz, C. H. *Acta Crystallogr.* **1989**, *B45*, 390.
- Némethy, G.; Printz, M. P. *Macromolecules* **1972**, *5*, 755.
- McNamara, L. M. A.; Andrews, M. J. I.; Mitzel, F.; Siligardi, G.; Tabor, A. B. *J. Org. Chem.* **2001**, *66*, 4585.
- Miller, S. J.; Blackwell, H. E.; Grubbs, R. H. *J. Am. Chem. Soc.* **1996**, *118*, 9606.
- Pernerstorfer, J.; Schuster, M.; Blechert, S. *J. Chem. Soc., Chem. Commun.* **1997**, 1949.
- Ravi, A.; Venkataram Prasad, B. V.; Balaram, P. *J. Am. Chem. Soc.* **1983**, *105*, 105.

MA012043L